

**How to Cite:**

Singh, H., Goyal, H., Singh, M., & Raj, R. (2022). Wind interference effect on a hexagonal-shaped high building with orifices. *International Journal of Health Sciences*, 6(S1), 8963–8982.  
<https://doi.org/10.53730/ijhs.v6nS1.7040>

# Wind interference effect on a hexagonal-shaped high building with orifices

**Harmanbir Singh**

Undergraduate Student, Department of Civil engineering, Delhi Technological University (DTU), Delhi, India

**Harsh Goyal**

Undergraduate Student, Department of Civil engineering, Delhi Technological University (DTU), Delhi, India

**Mayank Singh**

Undergraduate Student, Department of Civil engineering, Delhi Technological University (DTU), Delhi, India

**Ritu Raj**

Assistant Professor, Department of Civil Engineering, Delhi Technological University (DTU), Delhi, India

Corresponding author email: [rituraj@dtu.ac.in](mailto:rituraj@dtu.ac.in)

**Abstract**---This research examined at how the wind load and pressure on a tall hexagonal structure varied as the apertures changed. Wind angles ranging from 0 to 90 degrees with a 30-degree gap were employed in various situations. The distance between the interference building and the model building was also gradually increased, at 50mm intervals, from 50mm to 200mm. The major building model was examined at a scale of 1:500. The validity of the ANSYS CFX package was also evaluated using a rigid model with dimensions of 100mm x 100mm and a height of 700mm. The  $k-\epsilon$  -turbulence model was used in the study, which was carried out using Computational Fluid Dynamics (CFD) and the ANSYS CFX software package. To demonstrate the link between distinct scenarios, interference factors (IF) and contours were employed. Interfering buildings' impacts on the hexagonal-shaped building are explored. The pressure coefficient of the faces rises as the distance between the interference building and the model building grows. The impacts of apertures on the model building were also examined, with 5-20% openings given.

**Keywords**---Hexagonal-Shape Building, ANSYS (CFX), Wind Pressure Coefficient, Contours, Interference Factor

## **Introduction**

The introduction of new technologies and the pace of scientific advancement have resulted in a growth in the height, width, and scale of structures, making them even more vulnerable to the impacts of wind. As a result, the influence of wind loads on these sorts of structures becomes increasingly critical [1]. In this work, wind loads on the model structure were first analysed, and then the change in wind loads was investigated when openings were added to our model.

Currently, various research have been conducted utilising computational fluid dynamics (CFD) to investigate the impacts of wind on tall buildings. ANSYS (CFX) is a popular tool for analysing wind load on many types of constructions. Buildings with complex forms may also be simulated for numerical analysis, and the shape can be subdivided into various smaller pieces using proper meshing [2]. The research [3] investigated the mean pressure coefficient of a 'E' plan shaped tall building experimentally and computationally. Wind tunnel testing was used for experimental purposes, while CFD simulation was used for numerical analysis. These two tests were found to be in good agreement with one another.

Another study [4] conducted focused on the numerical analysis of tall structures utilising the Commonwealth Advisory Aeronautical Council (CAARC) building model. In the investigation, a numerical data comparison with measurements in a boundary wind tunnel revealed that an accurate time-dependent analysis is critical. The study [5] looked on differences in the stress and pressure coefficients of a tall building with an unsymmetrical or uneven 'E' plan form.. Again, experimental and numerical analyses were conducted utilising wind tunnel testing and CFD, and they were found to be in good agreement with one another. They determined that along wind hits had the largest positive force and pressure coefficients because the surface area is greater and the most wind energy is wasted on the frontal surface.

The current Indian Standard Code for wind loads over structures includes information on characteristics such as pressure fluctuation and force coefficients. However, when openings are supplied to irregular buildings, it fails to handle the intricacies of wind loads over them [6]. The major goal of this research is to examine wind loads over isolated structures as well as the influence of interference when a second building is provided during wind testing with openings of 10-15%.

## **Methodology**

### **Model Shape Selection**

The initial stage was to decide on the structure's form. Because several research on three and four-sided buildings have been conducted, the hexagonal shape was chosen for a realistic and distinct analysis [7,8,9].

### **Model Structure**

Using AutoCAD software, a 3D model of the building was constructed. The suitable height: width ratio was chosen based on cases of the IS 875 (Part 3) 2015 [6].


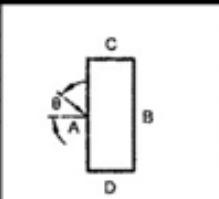

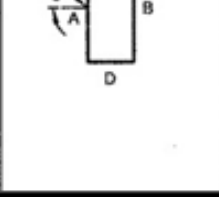

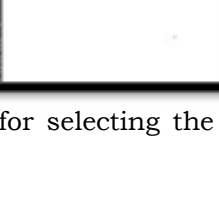
$\frac{h}{w} \geq 6$	$\frac{l}{w} = \frac{3}{2}$			0	+0.95	-1.85	-0.9	-0.9	} 1.25
				90	-0.8	-0.8	+0.9	-0.85	
	$\frac{l}{w} = 1.0$			0	+0.95	-1.25	-0.7	-0.7	} 1.25
				90	-0.7	-0.7	+0.95	-1.25	
	$\frac{l}{w} = 2$			0	+0.85	-0.75	-0.75	-0.75	} 1.25
				90	-0.75	-0.75	+0.85	-0.75	

Figure 1: Describes the criteria for selecting the appropriate height: width ratio using IS 875 (Part 3): 2015 [6]

The structure that is being simulated in this study is explained in the next chapter. It displays all of the calculations, including the proportion of openings in the structure, as well as its form and size.

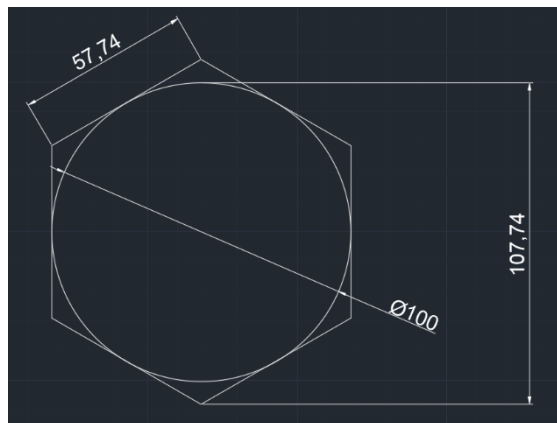


Figure 2: Top view of Model Building

The original height of the building is taken as 350 metres and the diameter of the circle is taken as 50 metres. The scale we chose for this study is 1:500 and thus the new dimensions for height and diameter become 700mm and 100mm respectively. Wall thickness of 1.2mm is taken.

### Openings

Total area of the building	=	Area of roof + Area of walls
	=	8661.74603 + 242508
	=	251170 mm <sup>2</sup> approximately.
Area of the openings	=	42000 mm <sup>2</sup>
Percentage of openings	=	16.72%
Size of a openings	=	40 X 25
Openings on a side	=	7

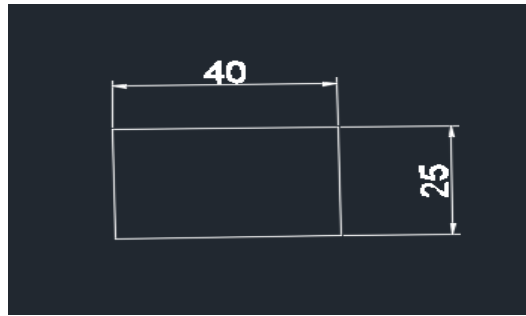


Figure 3: Dimensions of Openings

### Modelling in AutoCAD

We utilised AutoCAD software to create the models. We employed a variety of workstation stations, including drafting and annotations, as well as 3d Basics. The two photos show the realistic and 2D wireframes of the model creation. The same design was used for both the model and the interference buildings.

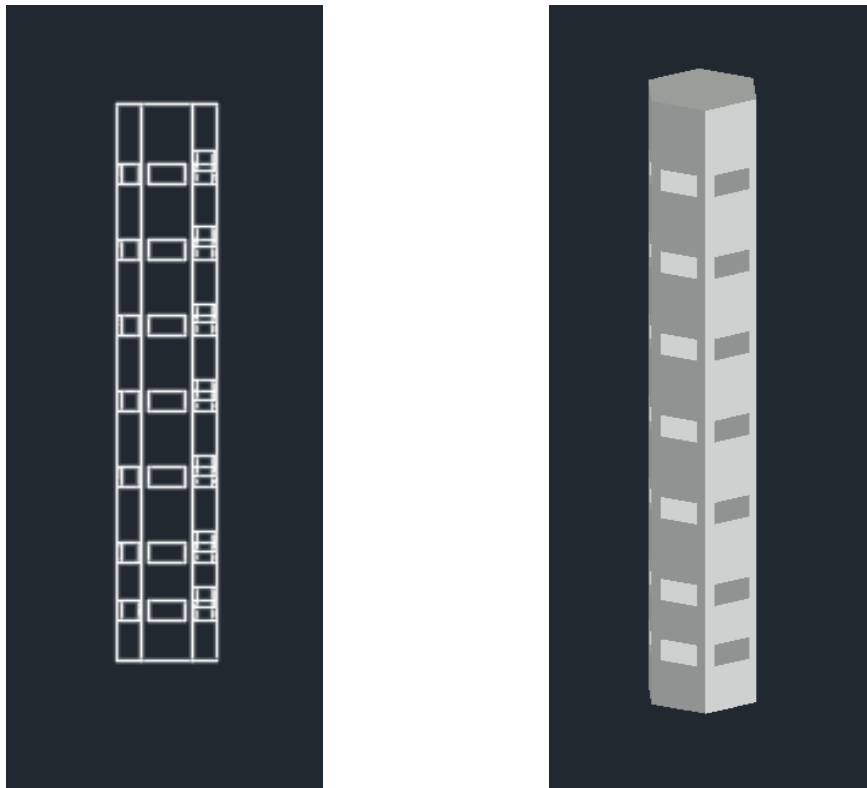


Figure 4: Includes the 2-D wire frame and realistic view of the model building which includes where openings have also been depicted.

### Validation using ANSYS

The ANSYS CFX Program required to be confirmed before starting with the in-depth numerical examination. This requires the establishment of a domain.

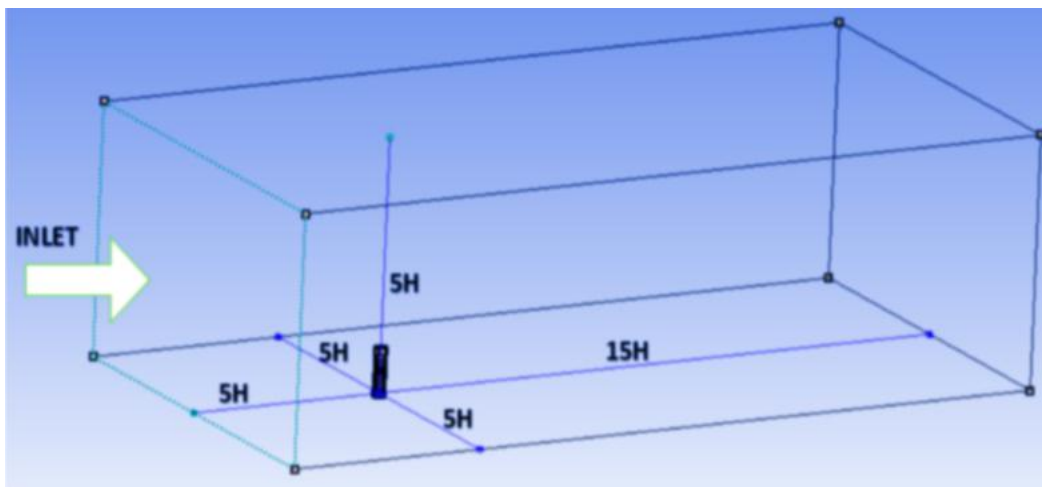


Figure 5: Describes the domain utilized for ANSYS validation.

The wind tunnel setting employed by [7] in their experimental investigation was like this region. The graph (Figure 6) displays the variability of velocity and turbulence intensity over the area and is equivalent to [7]

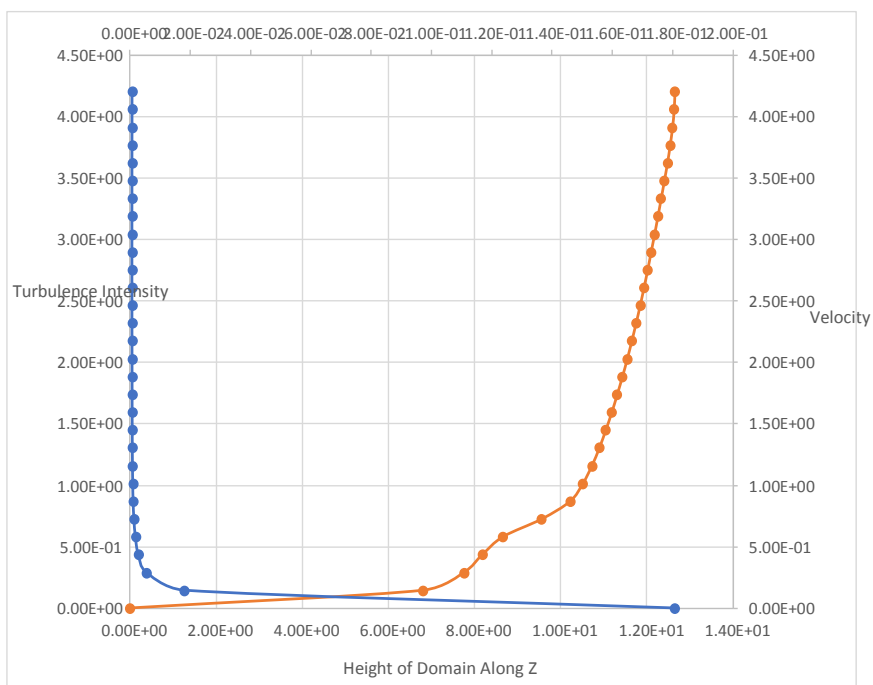


Figure 6: The fluctuation of velocity and turbulence intensity throughout the region is shown.

The model with L/W ratio one was validated in the domain using the k-epsilon [10] and SST [11] turbulence models discussed above. Wind impacts at  $0^\circ$  were explored for the models, and the results were compared to IS 875 (Part 3): 2015 [6].

### **Domain**

The domain (Figure 5) was created in compliance with the parameters of [12]. The intake and outflow distances were calculated to be  $5H$  and  $15H$ , respectively, where  $H$  represents the height of the building model. Both the top clearance and the side aspect were rated  $5H$ . As originally indicated, the length scale was changed to 1:500. This domain size is large enough to allow for the formation of vortices while avoiding the wind. The main causes of numerical simulation inaccuracy are the interference effects of the side and top faces. Reverse flow may occur due to a shortage of space in the outer direction, hindering the convergence of the CFD analysis. These can be prevented by following the advice of [8,12].

### **Meshing**

The meshing of the domain was done with tetrahedral components (Fig. 7). This is where 0.2-meter-diameter elements were made. To properly measure the wind characteristics, more delicate meshing was used around the building model. Face scaling was the name of the game, and the element size was 0.05 metres. To ensure a steady flow, mesh inflating was erected around the outside of the structure. Mesh inflation has a total of 20 layers to choose from.

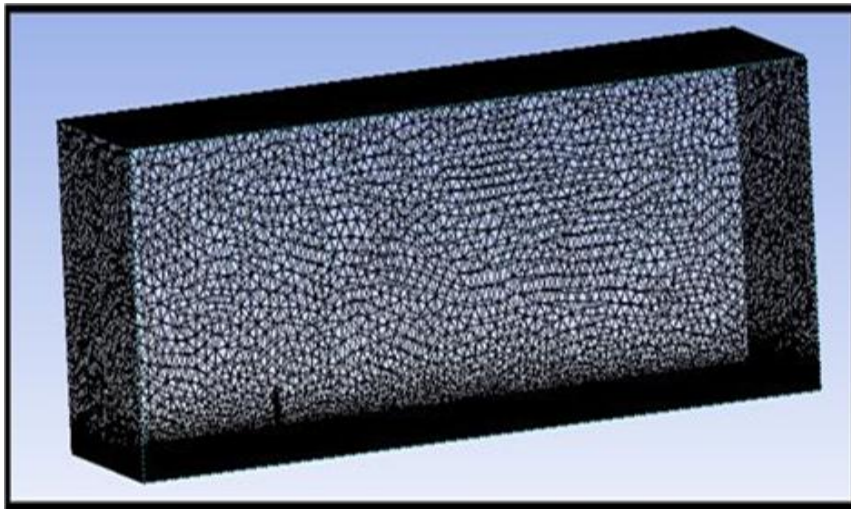


Figure 7: Shows the domain meshing, which was done with tetrahedral components

### **Contours**

Contours are defined as shadowing on the simulating body, with various hues representing different values of the contour's parameter. The value increases as the contour becomes darker, and lowers as the shade becomes lighter.

We plotted the contour for  $C_p$  values in this investigation.  $C_p$  is the pressure coefficient, which represents how much pressure is applied and in which direction it is exerted. The negative sign reflects suction force in the opposite direction of the wind, whereas the positive sign represents force in the same direction as the wind.

A legend is always supplied on the side to provide us with the values representing different colours so that we may know which colour represents which value. The photographs below show the isolated building's faces A and B, which have sixteen percent openings.

The numbers on the legend show that face A on the front side has positive values, indicating that force is applied in the direction of the wind, but face B on the rear side has a negative  $C_p$  value, indicating the development of a tiny vortex on the back side of the structure.

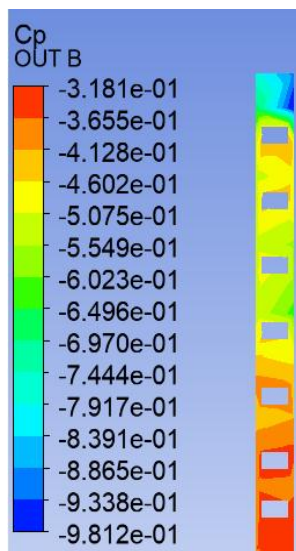


Fig 8:  $C_p$  of Face A

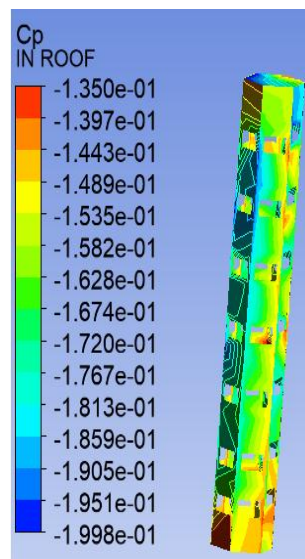


Fig 9:  $C_p$  of Face B

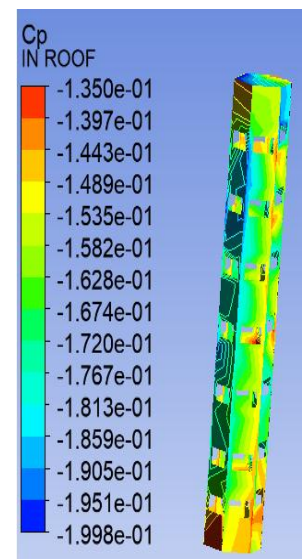


Fig 10: Contours of Inside Building

As the structure rotates, the face that confronts the wind direction experiences significant force, causing the force on face B to decrease and become less negative. This demonstrates that the face that facing the wind always feels the most pressure. When the building is rotated 30 degrees, the pressure is split across the two sides, A and D, indicating that this orientation is preferable than the one at 0 degrees.

Because all of the legend numbers are negative, the outlines of the inside building depict the suction force. The rotation of the building has essentially little influence on the interior structure since the total internal pressure of all the faces is almost constant.

The photographs below demonstrate that the value of  $C_p$  grows as the distance between the buildings increases, however we can detect a fall in  $C_p$  value between

100mm and 150mm spacing, which might be due to the creation of a vortex between the buildings, which lowers the  $C_p$  values. As the distance goes above 150mm, the effect of interference building begins to disappear.

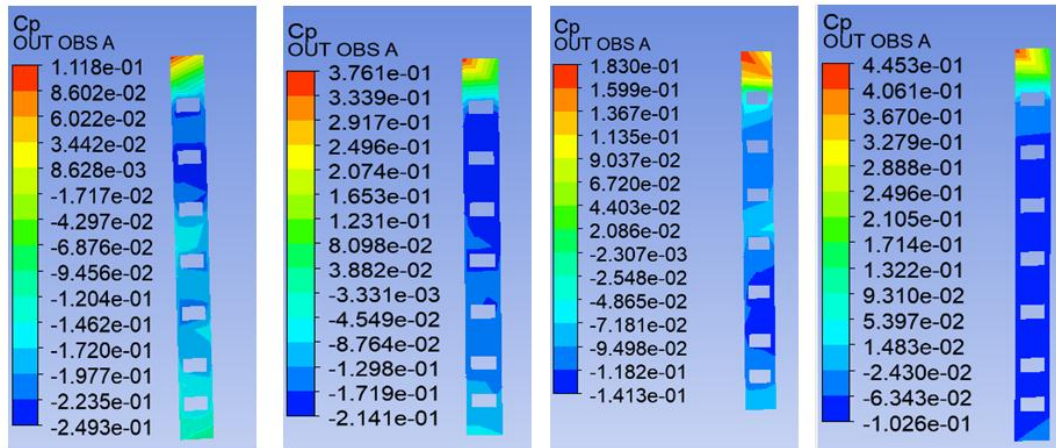


Figure 11: Contours of Face A for different spacing in ascending order.

Face B, on the other hand, has a normal rise in  $C_p$  values. The  $C_p$  value of this face is about half that of the isolated structure. This demonstrates that the existence of interference structures lessens suction force applied on that face.

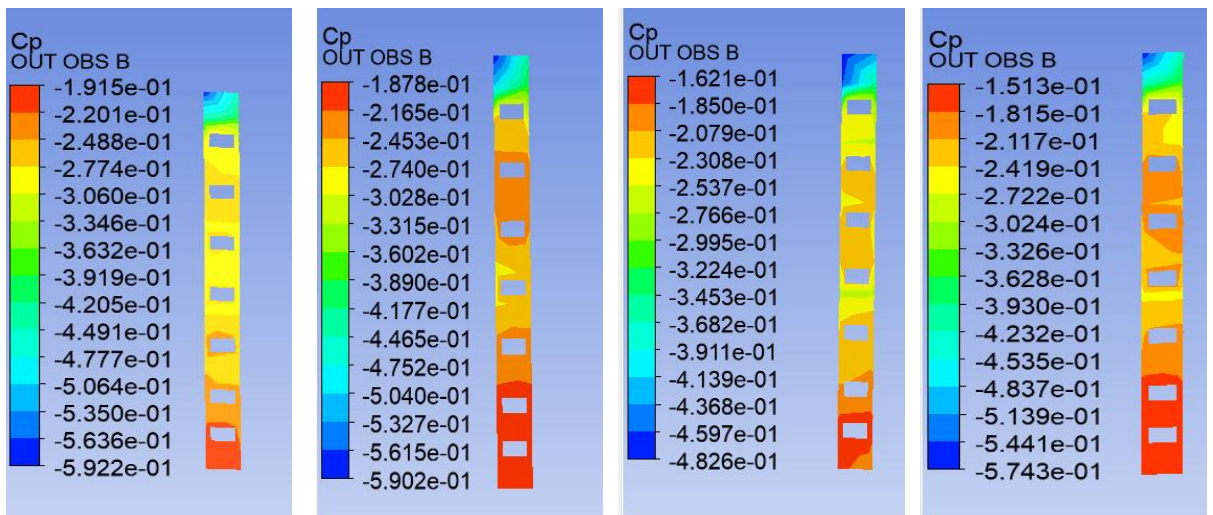


Figure 12: Contours of Face B for different spacing in ascending order



The photos below indicate that the presence of the interference building has greatly lowered the internal pressure of the building. Though increasing the distance increases the internal pressure, the increase is very minimal in all four circumstances.

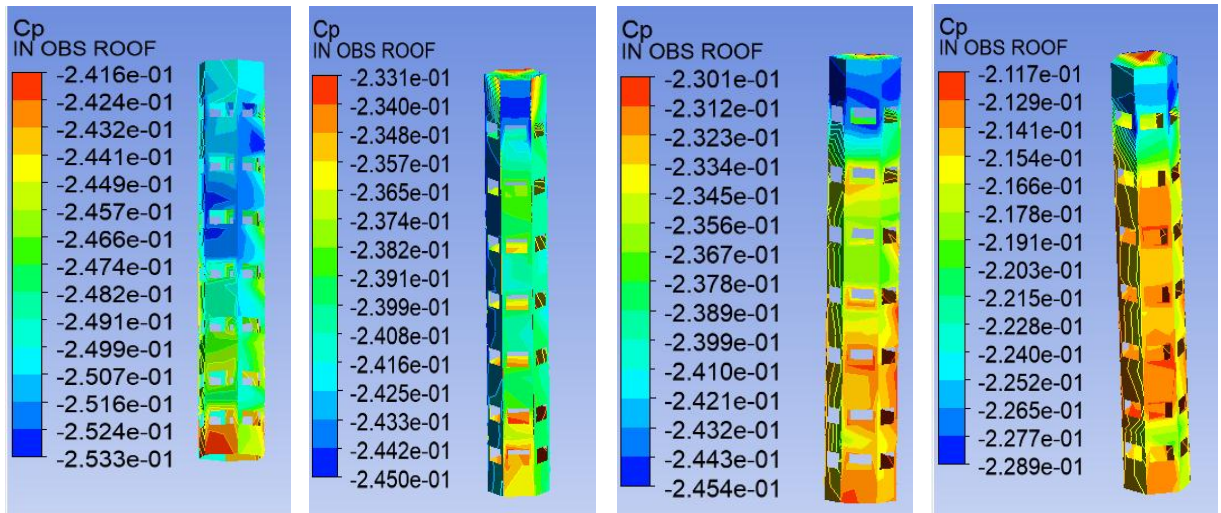


Figure 13: Contours of Internal Faces for different spacing in ascending order

### Streamlines

Streamlines are a visual representation of wind particles and how they will flow after they are halted by a structure. This animation vividly depicts how the wind would travel around the structure. This provides a clear picture of the vortex creation and aids in understanding the variety in  $C_p$  values.

The streamline perspective of the isolated building is displayed, which demonstrates the creation of a vortex on the back side of the building, resulting in very little pressure on the backside. This explains why suction force forms on the Face B.

A vortex forms between the buildings, which multiplies as the distance between them climbs to 150 mm, causing the  $C_p$  value of face A to fall as the distance increases. Because the vortex generated at 200 mm is modest, the  $C_p$  value on Face A rises. An increase in the spacing and intensity of the vortex formation inside the observation building is seen by an increase in the internal pressure of the building.

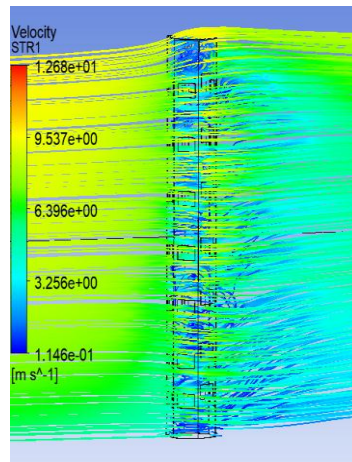


Figure 14 Streamline of Isolate Building

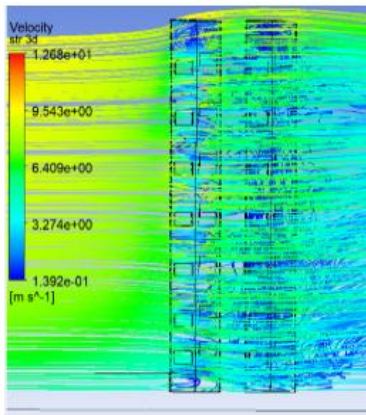


Figure 15: Streamline of 50mm spacing

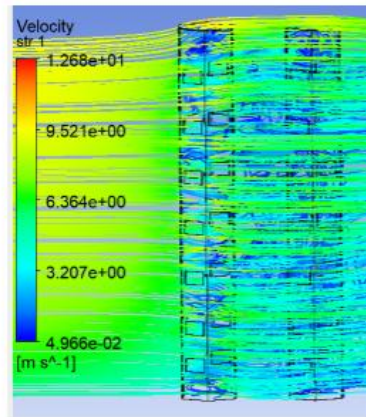


Figure 16: Streamline of 100mm spacing

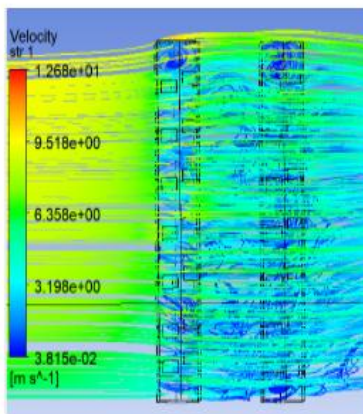


Figure 17: Streamline of 150mm spacing

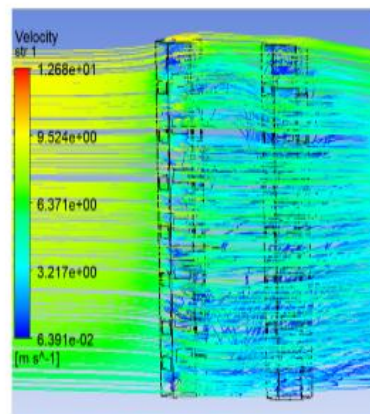


Figure 18: Streamline of 200mm spacing

## Results and Discussions

The results that we found by studying various graphs and calculating the  $C_p$  values are mentioned below.

### $C_p$ Values

The Pressure coefficient values for each face of the instrumental building is calculated using the expression given below.

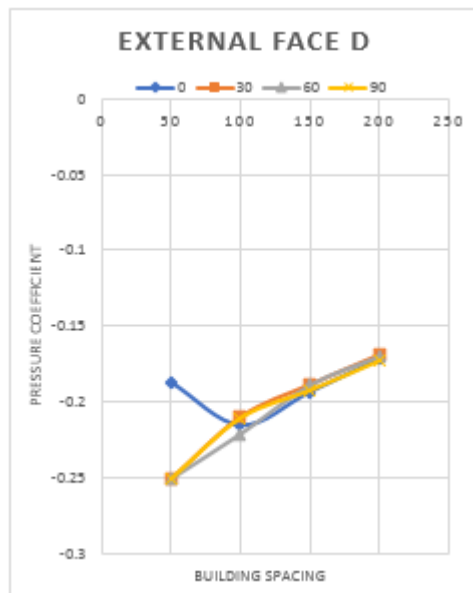
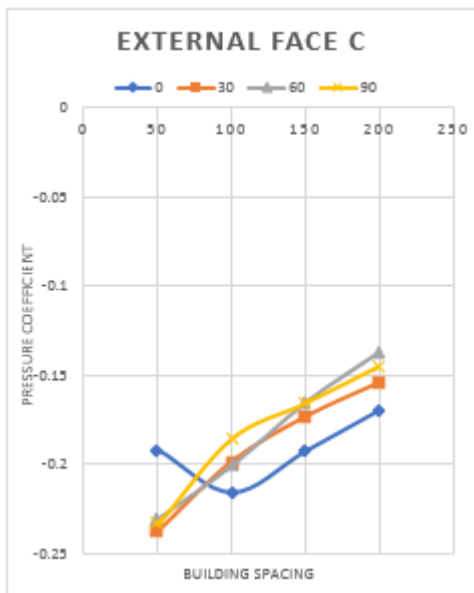
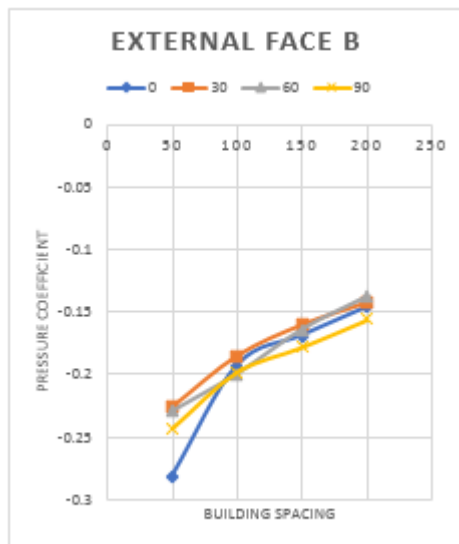
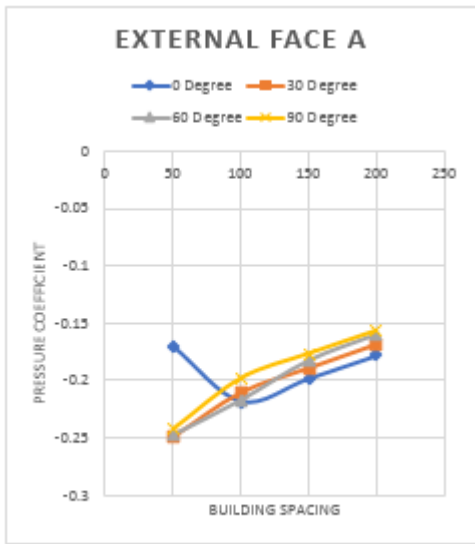
$$C_p = \text{Pressure} / (0.5 * \rho * u_{\text{Ref}}^2)$$

Where Pressure denotes the actual wind pressure,  $\rho$  denotes air density, and  $u_{\text{Ref}}$  is the reference velocity at the building height. The external pressure coefficients,  $C_p$  (facial average value), for the model's many faces [8].

The graphs for each and every face is plotted for all its angle to see the variation on how the  $C_p$  values changes as the instrumental building rotates. The conclusions drawn from the graphs are mentioned below.

It can be observed that as the distance between the interference building and the observational building grows, so does the value of  $C_p$ , with the exception of Face A at 0 degree. This might be due to vortex development when the distance between the buildings increases from 50mm to 100mm. As the distance grows, the  $C_p$  becomes less negative as the vortex's impact diminishes. Because of the creation of a vortex behind the observational building, Face B has the largest negative  $C_p$  value in the situation of 0 degree at 50mm distance.

Faces C and D are next to face A and hence have graphs that are almost identical. This also implies that faces E and F will have the same trendline as face B. Because there is considerable vortex formation, suction force rises, and therefore the  $C_p$  values on Faces C and D become increasingly negative as the distance grows in the case of 0 degrees, but the converse happens on Faces E and F.



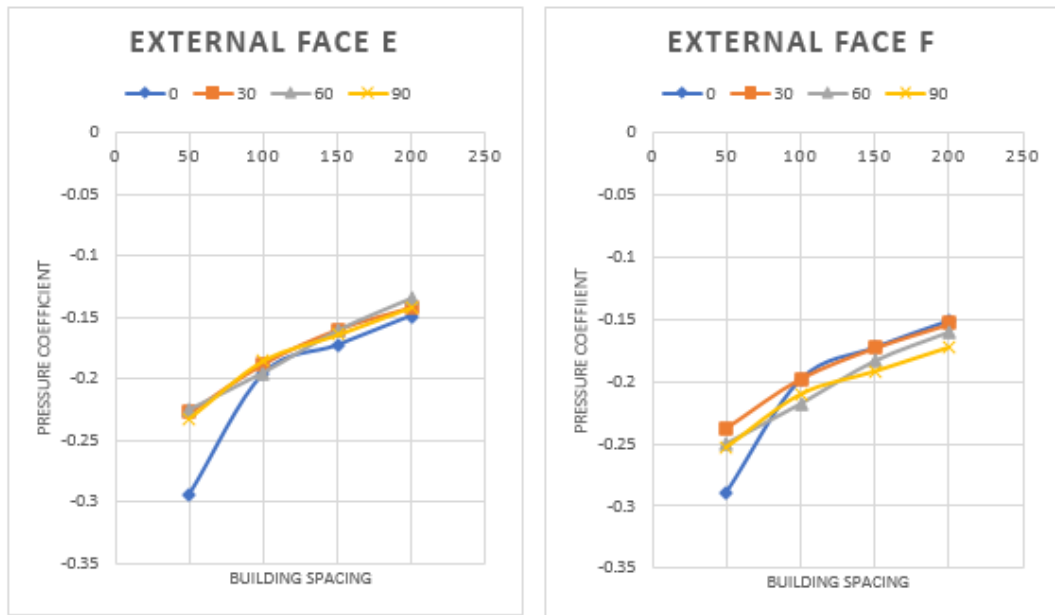
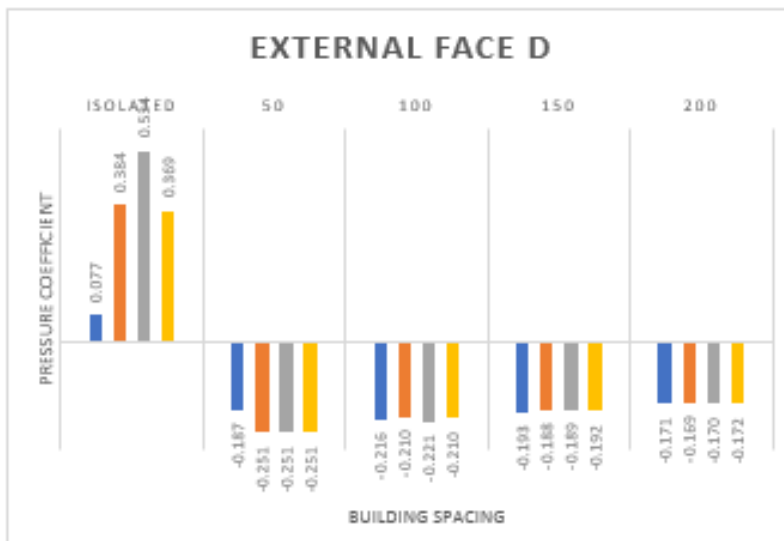
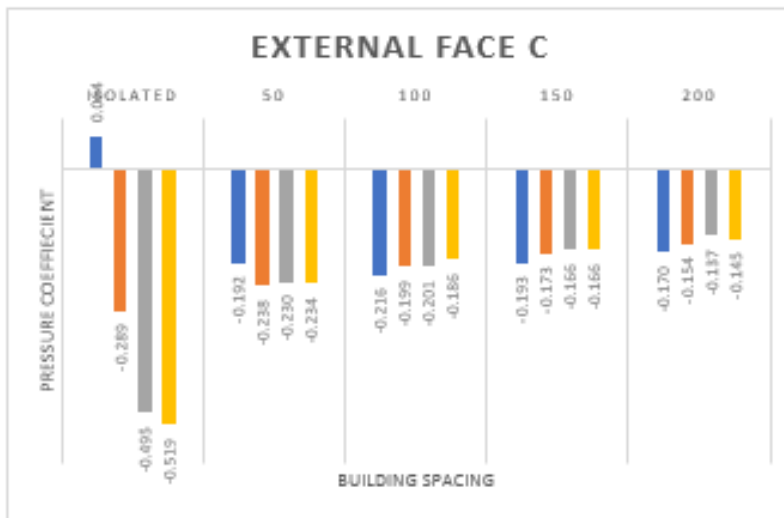


Figure 19 : Cp for Faces Comparison for Various Models Arranged at Different Angles

The graphs show the Cp values for each face in comparison to the isolated building. The graph of face A indicates that when the interference building is placed in front, the Cp values shift from positive to negative, indicating that the direction of force changes. The reduction in Cp values on Face B suggests that the interference building greatly reduces the pressure on both the windward and leeward sides.





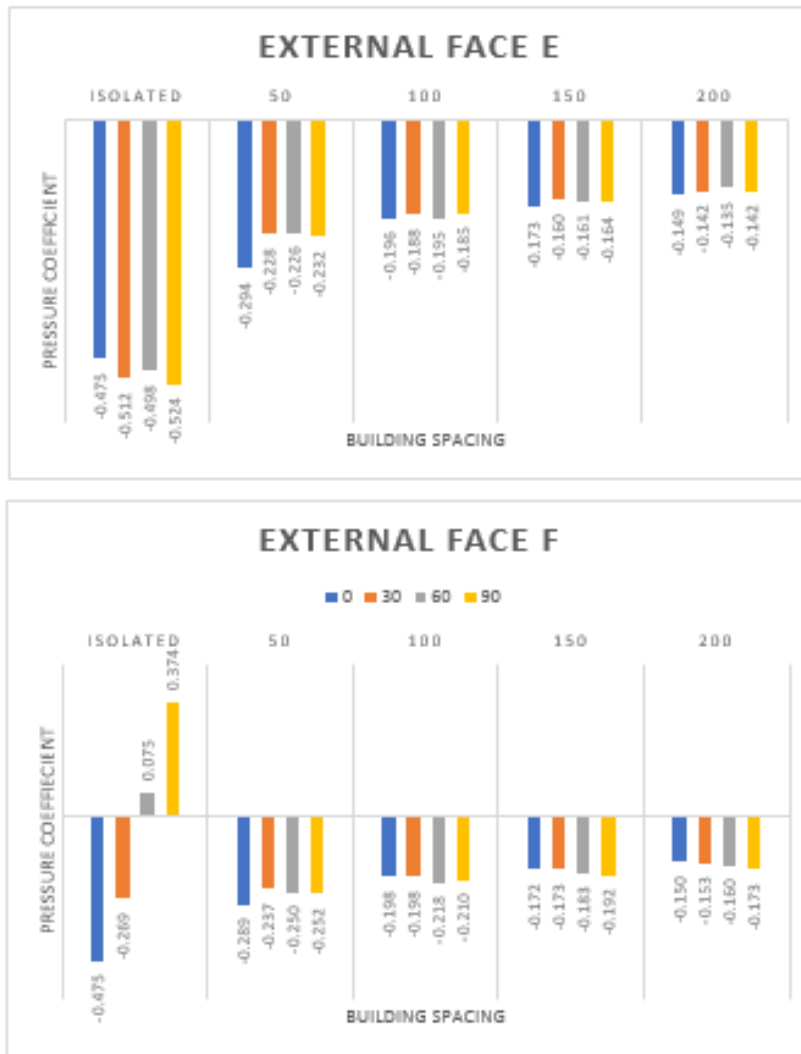


Figure 20: Cp values of the Isolated Building compared to other Interfering Models

**Interference Factor**

The interference effect is a metric that evaluates the strength of an obstruction in a fluid's path that prevents it from reaching the primary or test item. The more severe the interference, the higher the value of the interference factor. To investigate wind interference effects along wind direction, the force along the normal x-direction has been computed for all major models with varying configurations of interference construction sites and orientation. [9].



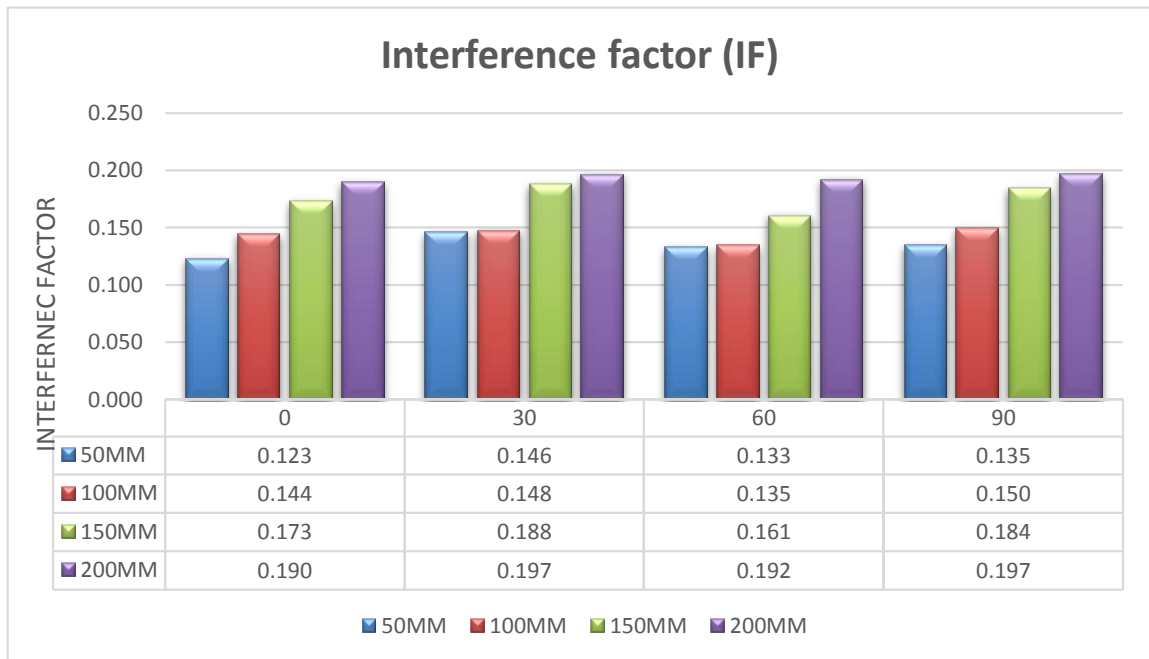


Figure 21: Graphical Representation of Interference Factor

$$\triangleright \text{IF} = \frac{\text{Force on Instrumental Building in the presence of Interference Building}}{\text{Force on isolated Instrumental Building}}$$

Graphing IF values for various distances and orientations is used to assess the interference influence on the instrumentation building. Values less than one imply that the observing building is shielded, whilst values greater than one indicate higher loading. [13].

It can be seen that all of the examples exhibit a shielding effect. The greater the value, the greater the shielding effect. Buildings with orientations of 0 and 60 degrees have a greater shielding effect than those with other angles. The first example, with a distance of 50mm between the buildings and a 0 degree orientation, has the most shielding impact, whereas the cases with a distance of 50mm between the buildings have the least shielding effect.

### Lift force and Drag force

For studying the variation of wind effects due to different wind angles we also plotted the various graph for  $C_{FX}$  and  $C_{FY}$  whose equations are given below:

$$C_{FX} = \frac{F_X}{0.5\rho L_Y H U_H^2} \quad C_{FY} = \frac{F_Y}{0.5\rho L_X H U_H^2}$$

- $C_{FX}$  and  $C_{FY}$  are the force coefficients of the whole building along X and Y directions, respectively

- $F_X$  and  $F_Y$  are the total forces over the building along the X- and Y-direction respectively
- $\rho$  is the density of wind;  $U_H$  is the reference velocity at the building height
- $L_X$  and  $L_Y$  are the projected length of building along to the X and Y axes, respectively
- $H$  is the height of the building [8].

Air resistance, often known as drag, is a force created by air that operates in the opposing direction of an item moving through it. It is the point at which air particles collide with the front of the item, slowing it down. The higher the surface area, the greater the number of air particles that impact it and the greater the resistance. The drag coefficient is proportional to the drag force exerted on the structures.

The drag coefficient is inversely related to the density of the fluid, i.e., water has a larger drag coefficient than air. The drag coefficient is inversely related to the fluid velocity.  $C_{FX}$  stands for drag force. Any upward pressure given to a structure that has the ability to raise it relative to its surroundings is referred to as an uplift force. Pressure from the ground below, wind, surface water, and other variables can all create uplift forces. Lift force is indicated by the symbol  $C_{FY}$  [14].

As can be observed, the greater the surface area, the greater the drag force, and hence the examples with angles 30 and 90 have higher drag force than the other two angles. Also, as the distance rises, the influence of the vortex decreases, and so the drag force increases.

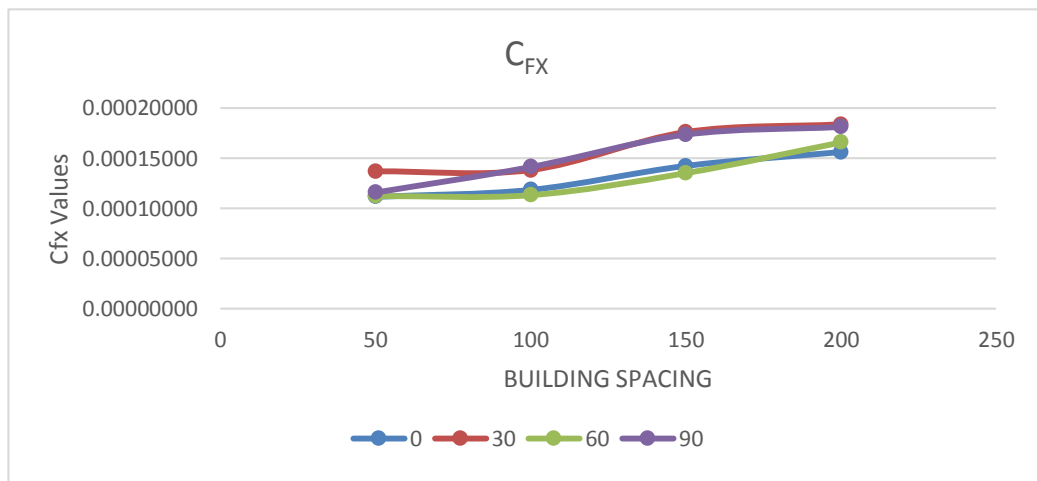


Figure 22.1: Graph of  $C_{FX}$

Unlike  $C_{FX}$ ,  $C_{FY}$  shows the unusual trend. The maximum  $C_{FY}$  is applied to a building with a 30 degree orientation, while the lowest is specified by a 60 degree orientation. Except for the 30 degree inclination, all of the trend lines follow a similar pattern.  $C_{FY}$  rises in all orientations when we proceed from 50mm to 100mm spacing, except in 30 degrees direction due to the creation of a vortex. The maximum  $C_{FY}$  force is applied to the case with 200mm spacing and a 30

degree orientation, while the lowest is applied to the case with 50mm spacing and a 60 degree orientation.

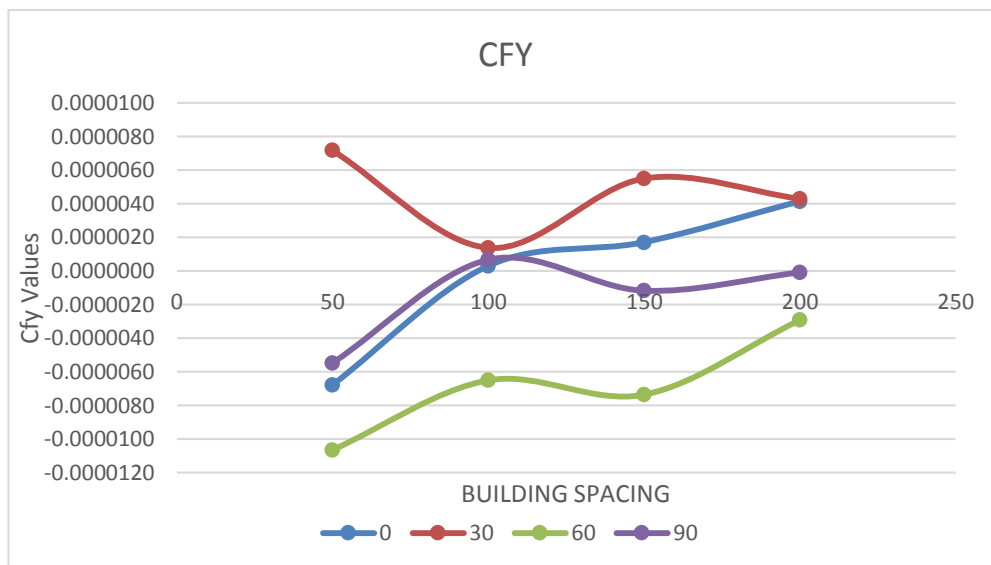


Figure 22.2: Graph of C<sub>FY</sub>

## Conclusions

The primary conclusions of this current study on the "hexagonal" plan shaped high structure with openings are as follows.:

- The internal pressure coefficient was discovered to vary as the model building was rotated based on the contours. The streamline diagrams also revealed that the majority of the air was trapped between the buildings owing to the holes.
- The streamline diagrams of the building show the formation of a vortex on the rear side of the structure, which grows in size as the distance between the interference and reference buildings grows.
- The influence of interference on the instrumentation building was assessed. Values less than one showed that the observing building was shielded, whilst values greater than one indicated higher loading.
- The highest shielding effect is seen when our instrumental building is positioned at 50mm and with a 0 degree angle.
- C<sub>FX</sub> has the same pattern as C<sub>FY</sub>, but C<sub>FY</sub> exhibits an unusual tendency. When we increased the distance from 50mm to 100mm, C<sub>FY</sub> increased in all orientations except 30 degrees due to the formation of a vortex. The case with 200mm spacing and a 30 degree orientation produced the greatest C<sub>FY</sub> force, whereas the case with 50mm spacing and a 60 degree angle produced the least.

## References

1. Gu M, Quan Y. Across-wind loads and effects of super-tall buildings and structures. *Science China Technological Sciences*. 2011 Oct;54(10):2531-41.
2. Kumar A, Raj R. Study of Pressure Distribution on an Irregular Octagonal Plan Oval-Shape Building Using CFD. *Civil Engineering Journal*. 2021 Oct 1;7(10):1787-805.
3. Bhattacharyya B, Dalui SK. Investigation of mean wind pressures on 'E' plan shaped tall building. *Wind and structures*. 2018 Feb 1;26(2):99-114.
4. Dagnew AK, Bitsuamalk GT, Merrick R. Computational evaluation of wind pressures on tall buildings. In 11th American conference on Wind Engineering. San Juan, Puerto Rico 2009 Jun 22.
5. Bhattacharyya B, Dalui SK. Along and across wind effects on irregular plan shaped tall building. In *Advances in Structural Engineering 2015* (pp. 1445-1460). Springer, New Delhi.
6. "IS (Indian Standard). 2015. Indian standard code of practice for design wind load on building and structures. IS 875 (Part 3). New Delhi, India: IS."
7. Mukherjee S, Chakraborty S, Dalui SK, Ahuja AK. Wind induced pressure on 'Y' plan shape tall building. *Wind & structures*. 2014;19(5):523-40.
8. Sanyal P, Dalui SK. Effects of side ratio for 'Y' plan shaped tall building under wind load. In *Building Simulation 2021* Aug (Vol. 14, No. 4, pp. 1221-1236). Tsinghua University Press.
9. Pal S, Raj R. Evaluation of wind induced interference effects on shape remodeled tall buildings. *Arabian Journal for Science and Engineering*. 2021 Nov;46(11):11425-45.
10. Jones WP, Launder BE. The prediction of laminarization with a two-equation model of turbulence. *International journal of heat and mass transfer*. 1972 Feb 1;15(2):301-14.
11. Menter FR. Two-equation eddy-viscosity turbulence models for engineering applications. *AIAA journal*. 1994 Aug;32(8):1598-605.
12. Jensen G, Franke J, Hirsch C, Schatzmann M, Sathopoulos T, Wisse JA, Wright N. Impact of Wind and Storm on City and Built Environment-Working Group 2 CFD Techniques- Computational Wind Engineering. In conference; COST Action C14, Impact of Wind and Storm on City Life and Built Environment; 2004-05-05; 2004-05-07 2004.
13. Pal S, Raj R, Anbukumar S. Bilateral interference of wind loads induced on duplicate building models of various shapes. *Latin American Journal of Solids and Structures*. 2021 Jul 26;18.
14. Lin N, Letchford C, Tamura Y, Liang B, Nakamura O. Characteristics of wind forces acting on tall buildings. *Journal of Wind Engineering and Industrial Aerodynamics*. 2005 Mar 1;93(3):217-42.